

# HYDROMETEOR DISCRIMINATION IN MELTING LAYER USING MULTIPARAMETER AIRBORNE RADAR MEASUREMENT

H. Kumagai<sup>1</sup>, R. Meneghini<sup>2</sup>, and T. Kozu<sup>3</sup>

1. Communications Research Laboratory, Koganei Tokyo 184, Japan

2. NASA/GSFC, Code 975, Greenbelt, MD 20771

3. National Space Development Agency of Japan, Minato, Tokyo 105, Japan

## ABSTRACT

Results from multiparameter airborne radar/radiometer experiment (Typhoon experiment) are presented. The experiment was conducted in the Western Pacific in September 1990 with the NASA DC-8 aircraft in which a dual-wavelength at X band and Ka band and dual polarization at X band radar was installed. The signatures of dBZ(X), dBZ(Ka), LDR (Linear Depolarization Ratio) at X band and  $DZ = dBZ(X) - dBZ(Ka)$  are discussed for the data obtained in the penetration in the super typhoon Flo. Putting emphasis on discrimination of hydrometeor particles, some statistical feature in the brightband in stratiform rain is discussed.

## INTRODUCTION

Polarimetric radar is playing an significant role in examining micro physical process within rain cloud. It is greatly advantageous to discriminate various types of hydrometeor particles[1],[2]. To vertically profile the precipitation and to identify the melting height are especially important for the measurement of global rainfall (e.g., TRMM satellite). The importance can be seen by noting that a change in phase state causes a drastic change in Z-R relationship and in the attenuation so that a failure in identifying the phase results in large error in estimating the equivalent rain rate or liquid water content.

An airborne experiment using the dual-polarization and dual-frequency radar, along with several microwave radiometers was conducted in the Western Pacific in September 1990. One of objectives of this experiment is to make radar/radiometer measurement over rain to support the algorithm development and science studies for TRMM and other spaceborne weather sensors. A second goal is to test the capabilities of dual polarization from an airborne platform with near nadir viewing. The airborne radar, nominally nadir pointing, operates at frequencies at of 10 GHz (X band) and 34.45 GHz (Ka band). In addition, the X-band radar was modified to provide reception in the two orthogonal linear polarizations (H and V) for a fixed transmit polarization (H). The linear depolarization ratio (LDR) is obtained by switching the received polarization state on a pulse to pulse basis[3]. The results obtained in the experiment suggest that the airborne multiparameter radar can be used to distinguish among various types of hydrometers even at near-nadir incidence.

## MULTIPARAMETER RADAR OBSERVABLES

### LDR (Linear Depolarization Ratio)

Because of the change in geometry, dual-polarization measurements from spaceborne or airborne radar require special consideration. The differential reflectivity ratio ( $Z_{DR}$ ) is given as

$$Z_{DR} = 10 \log(Z_{ehh}/Z_{evv}) \quad (1)$$

Where  $Z_e$  is the equivalent radar reflectivity factor, and the first and second subscripts refer to the linear polarization state for reception and transmission, respectively. For vertical incidence,  $Z_{DR}$  in rain should be very close to zero because the oblate drops tend to be aligned with their symmetry axis along the vertical. Furthermore, even non-

spherical particles such as ice, snow or partially melted particles, if randomly oriented, also yield  $Z_{DR}$  values close to zero.

The linear depolarization ratio (LDR) which is given as

$$LDR = 10 \log(Z_{evh}/Z_{ehh}) \quad (2)$$

behaves differently. LDR can provide useful data even at vertical incidence for non-spherical particles with random orientation. This means that LDR is particularly useful in identifying regions of melting particles.

### Difference in radar reflectivity factor with frequency

When the attenuation of the radar radiowave is taken into account, the measured radar reflectivity factor  $Z_m$  is given as

$$Z_m = Z_e e^{-0.46 \int_0^r k ds} \quad (3)$$

where  $k$  and  $r$  are the attenuation coefficient and range to the scattering volume. In dual frequency observations, the measured radar reflectivity factors  $Z_m$  at the two frequencies generally differ. The primary reason for this is the effect of differential attenuation: if the attenuation at the lower frequency is negligible and the scattering is predominantly Rayleigh, then this difference is a measure of the cumulative path attenuation at the higher frequency. However, even in cases where the differential attenuation is small,  $Z_m$  will exhibit a frequency dependence as Mie scattering effects become important. In general as the particle size distribution shifts to larger sizes  $dBZ_e(X) - dBZ_e(Ka)$  will increase. The difference of  $dBZ_{ehh}$  at frequencies of X and Ka band is defined as

$$DZ_e = dBZ_{ehh}(X) - dBZ_{ehh}(Ka) \quad (4)$$

The difference of  $dBZ_{mhh}$  is given in the similar way as

$$DZ_m = dBZ_{mhh}(X) - dBZ_{mhh}(Ka) \quad (5)$$

Notice that  $DZ_e$  depends only on Mie scattering effects, whereas  $DZ_m$  depends on both Mie scattering and on the cumulative differential attenuation out to the radar range of interest.

## RESULTS

### Radar system parameters

The beamwidths of the antennas for the 10 GHz and 34.5 GHz channels are approximately the same and, for the typical altitude of 12 km, yield a spot size at the surface of about 1 km. The radar pulse duration of 0.5  $\mu$ s gives a nominal range resolution of 75 m. However, the return pulse is oversampled at a rate of 5 MHz. The PRF is 440 Hz. The data presented in this paper represent the sample average over a time window of about 2.4 sec which translates into 512 sample average for all the co- and cross-polarized X-band returns and co-polarized Ka-band return. The isolation between the horizontal and vertical X-band channels is determined primarily by the isolation of the antenna, which gives a minimum detectable LDR of about -30 dB[3].

91-72810/92\$03.00 © IEEE 1992

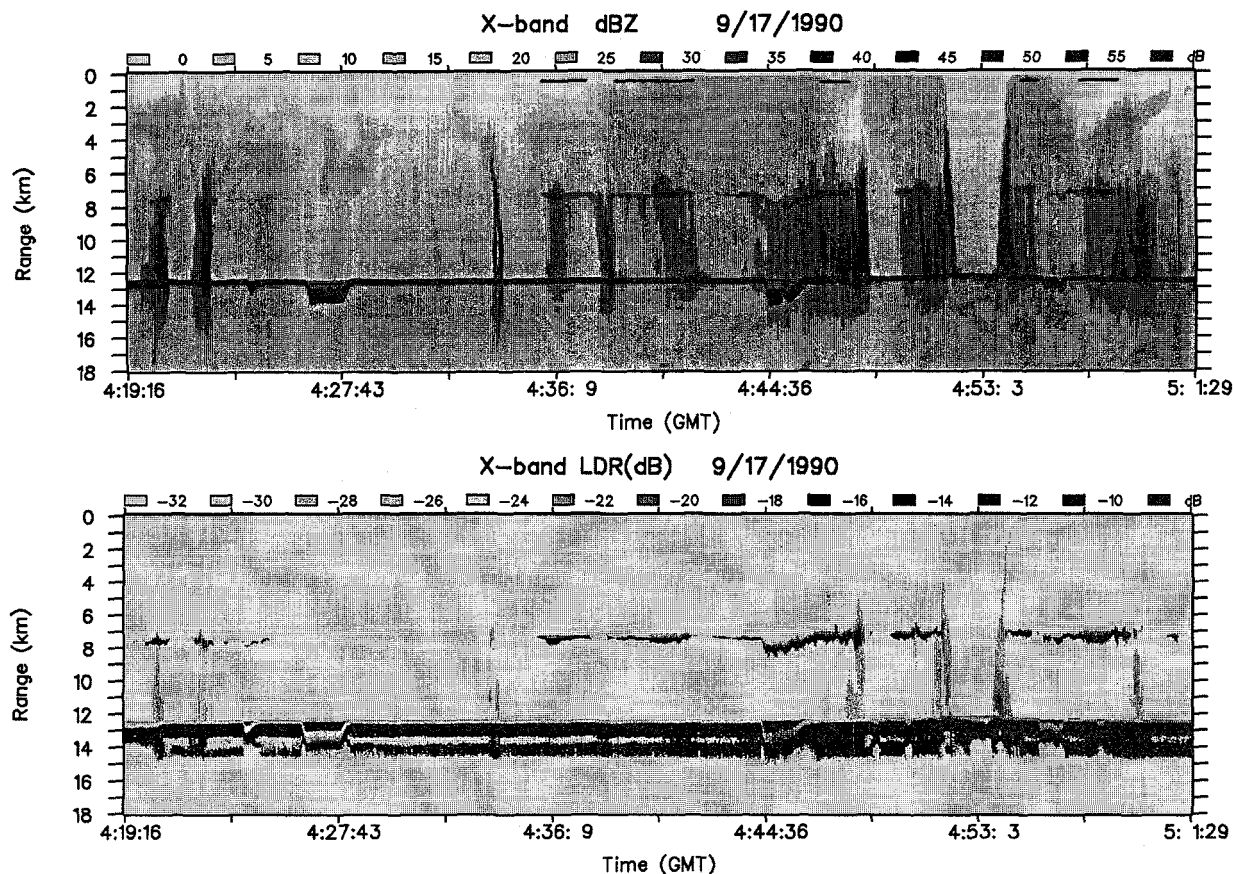


Fig.1: Range-time profiles of (a)dBZ(X) and (b)LDR obtained from the flight on September 17, 1990.

#### Range-time profiles of dBZ(X) and LDR

An overview of the data obtained from the flight on September 17, 1990 is shown in Fig. 1(a),(b). The aircraft flew over the super typhoon Flo and penetrated the eye at 4:52- 4:53 GMT at the height of 12.5 km. Figs. (a) and (b) show range-time profiles of X-band  $\text{dBZ}_{\text{mhh}}$  and X-band LDR, respectively. The LDR presented here is not based on (2) but is given as  $10\log(Z_{\text{mvh}}/Z_{\text{mhh}})$ ; in particular, a correction for attenuation is not made. The abscissa (time) also represents the horizontal distance that the aircraft flew. Although the flight path is not straight during time period shown in Fig. 1, the total abscissa (42 min) corresponds to the distance of about 630 km. The ordinate represents the range in km from the aircraft. The thick horizontal line at 12.5 km is the echo from sea surface. Those periods in Fig. 1 that exhibit an increase in the range of the surface and a broadening of the surface return correspond to aircraft banking maneuvers.

Fig.1(a) shows a 40 min segment of the 10 GHz radar data. During this period the aircraft overflowed several rain bands as well as the eye of super typhoon Flo centered at 4:52 GMT. Most of the rain is stratiform in nature with a clearly defined bright-band (melting layer signature) at a range of about 7 km (5.5 km above the sea surface). Even in the region close to the eye wall a bright-band signature is evident. The convective cells are compact. Consistent with previous observations, these convective cells tend to be present at the inner edges of the rain bands.

In Fig.1(b), LDR is plotted only for those points in which the cross polarization return power exceeds the receiver noise level. Above the sea surface, two types of LDR signatures can be seen. One is very high values of LDR within the melting layer, and confined to a 1 km range about the 0 C. Typical values of LDR in this region range from -15 dB to -10 dB. It is considered that eccentric or

irregularly shaped partially melted particles are responsible for this LDR signal. On the other hand, in convective cells and smaller sections of stratiform cells, an LDR is detected over a extended range. These values of LDR are lower than those in the melting layer with values between -25 dB and -20 dB. In the eye wall, a detectable LDR signature extends up almost to the aircraft height. Possible causes for this type of LDR are: large canting angles of the raindrops under strong wind condition, partially melted hydrometeors, propagation effects, or a combination of these factors.

#### Range profiles of observables

Fig. 2 shows an example of range profiles of  $\text{dBZ}_{\text{mhh}}(\text{X})$ ,  $\text{dBZ}_{\text{mvh}}(\text{X})$ ,  $\text{dBZ}_{\text{mhh}}(\text{Ka})$ , LDR, and  $\text{DZ}_m$  at 4:36:10 GMT. This observation was taken within the

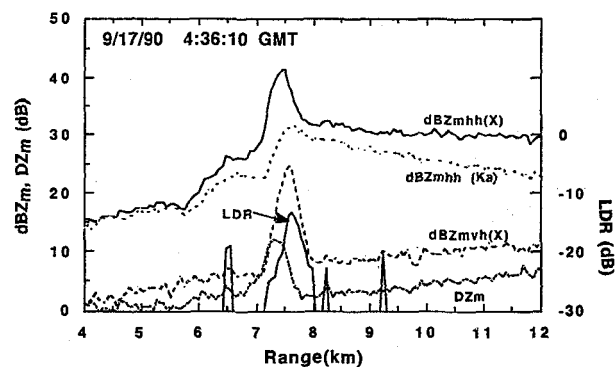


Fig. 2: Range profiles of  $\text{dBZ}_{\text{mhh}}(\text{X})$ ,  $\text{dBZ}_{\text{mvh}}(\text{X})$ ,  $\text{dBZ}_{\text{mhh}}(\text{Ka})$ , LDR, and  $\text{DZ}_m$  at 4:36:10 GMT on September 17, 1990.

intense portion of the stratiform cell shown in Fig. 1. The  $\text{dBZ}_{\text{mhh}}(X)$  curve in Fig. 2 shows a maximum at the melting layer which occurs at a radar range of 7.4 km (4.8 km above sea level). In contrast, the increase in  $\text{dBZ}_{\text{mhh}}(\text{Ka})$  is smaller than that in X band. The curve of  $\text{dBZ}_{\text{mvh}}(X)$  represents the receiver noise level except for a sharp increase in the ranges centered about the melting layer. Therefore, meaningful values of LDR are available only within these ranges, where the LDR exhibits a sharp increase up to a peak of -13 dB. We assume  $Z_e(X) = Z_m(X)$  here because of the cumulative attenuation at X band down to these ranges is small. The curve of  $\text{DZ}_m$  in Fig. 2 exhibits a local maximum in the melting layer. Most of this increase is caused by the effects of Mie scattering, namely, Mie scattering occurs at Ka band. The gradual and monotonic increase in  $\text{DZ}_m$ , which occurs below the melting layer, is due to the differential attenuation. We may suggest that the effective particle size becomes larger in the range where  $\text{DZ}_m$  has a maximum.

#### Melting layer statistics

Some statistical features of the melting layer in the stratiform rain are examined using the data shown in Fig. 1. The purpose is to examine the mutual-relationship among radar observables, such as peak values of  $\text{dBZ}_{\text{mhh}}(X)$ ,  $\text{dBZ}_{\text{mhh}}(\text{Ka})$ , LDR,  $\text{DZ}_m$ , and thickness of melting layer, which is defined as the interval over which  $\text{dBZ}_{\text{mvh}}(X)$  exceeds the receiver noise level. Because of the well-defined

nature of the LDR curve within the melting layer it can be used as a convenient way to define the vertical extent of the melting layer. The value of  $\text{dBZ}_{\text{mhh}}(X)$  at the rain top is used as a measure representing rain rate. We selected 74 data points from the time periods within the horizontal bars shown in the top of Fig. 1(a).

Two scatter plots are shown in Fig. 3(a)(b). In the first, the relation between  $\text{dBZ}_{\text{mhh}}(X)$  at the rain top and peak of LDR ( $\text{LDR}_{\text{max}}$ ) is shown (a). The correlation coefficient is low (0.28), which suggests that the  $\text{LDR}_{\text{max}}$  is weakly dependent on the rain rate. Similar calculations were performed using the  $\text{LDR}_{\text{max}}$ , the  $\text{dBZ}(X)$  maximum ( $\text{dBZ}(X)_{\text{max}}$ ) and the vertical extent of the melting layer ( $h_{\text{BB}}$ ). The correlation coefficients between  $\text{LDR}_{\text{max}}$  and  $\text{dBZ}(X)_{\text{max}}$ , and between  $\text{LDR}_{\text{max}}$  and  $h_{\text{BB}}$  are 0.45 and 0.39, respectively. As before, these low coefficients indicate a weak correspondence between these quantities. Fig. 3(b) shows a scatter plot between  $\text{LDR}_{\text{max}}$  and peak of  $\text{DZ}_m$  ( $\text{DZ}_m \text{ max}$ ), which shows a relatively high correlation coefficient of 0.62. Among the parameters which we examined between  $\text{LDR}_{\text{max}}$ , the highest correlation found is that between  $\text{LDR}_{\text{max}}$  and  $\text{DZ}_m \text{ max}$ . This fact may seem strange because  $\text{DZ}_m$  is primarily related to the particle size and refractive index, whereas LDR is related to the particle shape and orientation and refractive index. The result seems to indicate that there is a fairly high degree of correspondence between the volume and asphericity of the melting particles.

#### CONCLUSIONS

In this paper, results from an airborne radar experiment have been presented on the dual-polarization and dual-wavelength signature. We examined the LDR and  $\text{DZ}_m$  characteristics in the melting layer in stratiform rain. Statistical calculations on the parameters of the melting layer show that the correlation coefficient between the maxima of LDR and of  $\text{DZ}_m$  is relatively high. On the other hand, only weak correlations are obtained between the LDR maxima and other parameters such as  $\text{dBZ}(X)_{\text{max}}$ ,  $\text{dBZ}(X)_{\text{rain top}}$ , and  $h_{\text{BB}}$ . The high correlation between LDR and  $\text{DZ}_m$  seems to indicate a certain degree of correspondence between the particle volume and its eccentricity. To understand this relationship on quantitative basis requires modeling studies of the melting layer.

#### REFERENCES

- [1] V.N. Bringi, J. Vivekanandan, and D. Tuttle, "Multiparameter radar measurements in Colorado convective storms Part II: hail detection studies", *J. Atmos. Sci.*, **43**, 2564-2577, 1986.
- [2] I.R. Frost, J.W.F. Goddard and A.J. Illingworth, "Hydrometeor identification using cross polar radar measurements and aircraft verification", *25th Conf. Radar Meteor.*, 658-661, Paris, June 1991.
- [3] H. Kumagai, R. Meneghini, and T. Kozu, "Multi-parameter airborne rain radar experiment in the Western Pacific", *25th Conf. Radar Meteor.*, 400-403, Paris, June 1991.

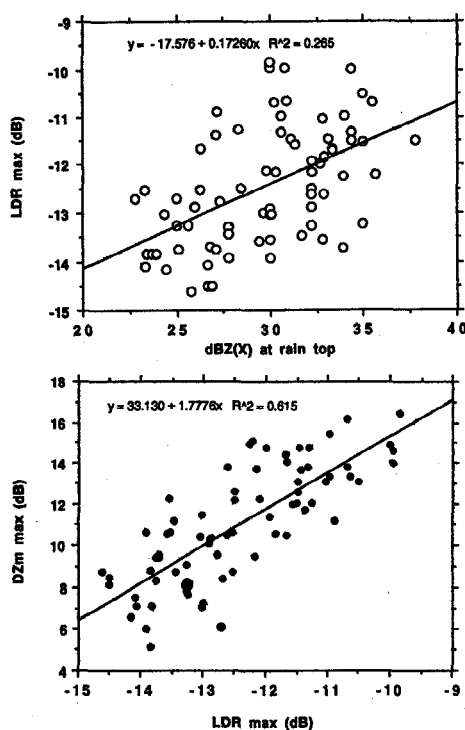


Fig.3: Scatter plots among melting layer quantities; (a) correlation between  $\text{dBZ}_{\text{mhh}}(X)$  at rain top and  $\text{LDR}_{\text{max}}$ , (b) correlation between  $\text{LDR}_{\text{max}}$  and  $\text{DZ}_m \text{ max}$ .